Deuteron nuclear magnetic resonance and dielectric study of host and guest dynamics in KOH-doped tetrahydrofuran clathrate hydrate

H. Nelson,[1] A. Nowaczyk,[1] C. Gainaru,[1] S. Schildmann,[1] B. Geil,[2] and R. Böhmer[1,*]
[1]*Fakultät für Physik, Technische Universität Dortmund, 44221 Dortmund, Germany*
[2]*Institut für Physikalische Chemie, Universität Göttingen, 37077 Göttingen, Germany*
(Received 29 March 2010; revised manuscript received 21 May 2010; published 11 June 2010)

The host as well as the guest dynamics in ion doped clathrate hydrates were studied via several deuteron nuclear magnetic resonance techniques and using broadband dielectric spectroscopy in conjunction with the application of large electrical fields. At a given temperature evidence for up to three relaxation processes was found for samples with mole fractions larger than 10^{-4} KOH. The two slower processes, unraveled via an electrical cleaning procedure, are similar to those detected on undoped samples in which they proceed on slightly longer time scales. The fastest process exhibits a weak temperature dependence except close to the transition into the low-temperature phase. Here, an incomplete proton order is established on the hydrate lattice and a residual orientational motion of the guest molecules could be detected at low temperatures. These results demonstrate the large degree of coupling between host and guest motions.

DOI: 10.1103/PhysRevB.81.224206 PACS number(s): 82.75.−z, 77.22.Gm, 82.56.−b, 64.60.Cn

I. INTRODUCTION

Clathrate hydrates continue to receive much attention due to their ability to allow for storage of molecules of various sizes.[1] In the present paper, we focus on tetrahydrofuran (THF) as a guest molecule. THF clathrate hydrates crystallize in the so-called sII structure slightly above 0 °C. They are dynamically disordered in several respects. On the one hand, the water molecules forming the host lattice perform a cooperative motion which is governed by the Bernal-Fowler ice rules. When detected on the μs time scale, e.g., by nuclear magnetic resonance (NMR) line-shape techniques, this motion can be observed to freeze in at temperatures near 200 K.[2,3] This freezing leads to a static proton disorder at low temperatures. The dynamics of the THF molecules, on the other hand, is largely unaffected by the proton dynamics on the lattice and the guests continue to perform a fast reorientational motion which, on the μs scale, slows down only below about 30 K.[4]

Nevertheless, the present results from NMR and from dielectric spectroscopy (DS) experiments demonstrate that the THF molecules can act as sensitive sensors of the behavior of the surrounding H_2O lattice, pointing to the importance of host/guest interactions. The starting point of the approach used in the present paper is the previously reported possibility that the dynamics of the host lattice can be accelerated dramatically by adding minute amounts of KOH (mole fraction from 10^{-4} to 10^{-3}) when growing the THF clathrate hydrates.[5] Near 70 K the doping induced speed up of proton motion on the H_2O lattice was reported to amount up to about 10 orders of magnitude.[6] This result suggests that sufficient protonic mobility persists down to temperatures at which the interaction energy between the proton species outweighs the thermal energy so that an ordered host structure can emerge. This phenomenon is not unique to clathrate hydrates. On the contrary, it was first discovered and studied for various phases of ice.[7] It has been argued that the K^+ and the OH^- defects act as catalysts for the dynamics on the H_2O lattice.[8,9] Along these lines ion doping has made it possible to generate proton ordered phases, e.g., ice *XI* from ice I_h.[10] The phenomenon seems general and applies to various other ice phases (see p. 373 of Ref. 7 and Ref. 11), for which the addition of ionic defects (typically on the 10^{-4} level) leads to proton-ordered phases.

KOH-doped THF clathrate hydrates have been investigated previously by calorimetry,[12] DS,[6,13] neutron scattering,[14] and thermal conductivity measurements.[15] From these works it is well known that KOH doping can lead to a first-order phase transition at a temperature near 62 K. In the course of this transition which occurs similarly also in acetone and 1,4-dioxane clathrate hydrates[16,17] an only incomplete proton order is established on the hydrate lattice. As discussed by Yamamuro *et al.*,[13] the remaining degree of proton disorder is hard to determine quantitatively on the basis of calorimetric data. This is because here only the *sum* of the transition enthalpies originating from the partial ordering of the proton lattice and from the unknown degree of ordering of the guest molecules is accessible.

One of the goals of the current ^{2}H-NMR study therefore is to determine the degree of ordering of the deuterated THF molecules (=TDF) in KOH doped $TDF\cdot 17H_2O$ clathrates. Our results can be compared to previous deuteron NMR data on the *un*doped THF clathrate hydrate.[2,3,18,19] Here, over a wide temperature range (50–200 K) Gaussian deuteron line shapes were observed for the guest molecules. Using a distorted octahedral jump model this line profile was linked to the proton disorder of the clathrate cages.[20] One of the consequences of that model is that the Gaussian line shapes should vanish to the extent to which the protons become ordered on the lattice of water molecules. Apart from checking this prediction, this situation enables the determination of the fraction of guests which remain disordered below the phase transition temperature.

In addition to investigating selectively guest deuterated crystals ($TDF\cdot 17H_2O$) we study the properties of selectively host deuterated samples ($THF\cdot 17D_2O$) doped with KOH and compare our NMR results with dielectric data. For ice I_h corresponding comparisons have yielded valuable insights

TABLE I. Compilation of sample compositions used for the present work. They are selectively deuterated as indicated. The nominal KOH mole fraction x and the method used for the study of the crystals are also given.

Composition	$x/10^{-4}$	Method
$THF \cdot 17D_2O$	1	DS/NMR
$TDF \cdot 17H_2O$	1.8	NMR
$THF \cdot 17D_2O$	5	DS
$THF \cdot 17D_2O$	10	DS/NMR

into the nature of the defect motion in these hydrogen-bonded networks.[21]

This paper is organized as follows: Next, some experimental details are given. Then, in Sec. III, we report on DS and NMR experiments performed to study the various relaxation processes that accompany the freezing dynamics on the water lattice. Sec. III B is devoted to phenomena related to the establishment of the low-temperature phase in the THF clathrate hydrates. Then, in Sec. III C the guest molecules are employed as sensitive sensors of the dynamics in that phase and of its partial order. After a general discussion in Sec. IV, which includes a detailed comparison with the behavior of KOH doped ice, we summarize our main findings in Sec. V.

II. EXPERIMENTAL DETAILS

Selectively deuterated single crystals were grown from aqueous THF solutions according to the procedure described previously,[20] except that KOH was added to the solution in appropriate amounts. Nominal doping levels (in the 10^{-4} to 10^{-3} range, see Table I) are given as mole fraction, $x = n(\mathrm{KOH})/[n(\mathrm{KOH}) + n(H_2O)]$, with $n = m/M_{\mathrm{mol}}$ denoting the number of molecules and M_{mol} the molar mass. There is a tendency of ice-like (as well as other) solids to "push" impurities diffusively out of the crystal lattice if the sample is kept just below the melting point.[8,22,23] Although this situation was usually avoided, it cannot be excluded entirely that the actual KOH content in some instants is somewhat lower than the nominal one.

For the NMR measurements the crystals were finely ground in an inert atmosphere and then hermetically sealed into glass tubes. The samples were stored in a liquid nitrogen vessel, transferred from there to the NMR radio-frequency coil as quickly as possible, and then inserted into the precooled cryostat. Other details of the NMR experiments and of the data processing are analogous to those described earlier,[20] except that now $\pi/2$ pulses in a somewhat larger range were used.[24]

The dielectric samples were grown from solutions that were in turn obtained by melting previously grown crystals. The dielectric measurements were carried out by recrystallizing these solution within dielectric cells which were constructed from invar and sapphire. The complex dielectric constant, $\varepsilon^* = \varepsilon' - i\varepsilon''$, was monitored with an excitation voltage of 1 V_{rms} using an α-analyzer from Novocontrol which covered the frequency range $10^{-2}\ \mathrm{Hz} \leq \nu \leq 10^{7}\ \mathrm{Hz}$. For the electrical purging procedure[25] described in Sec. III A 2, bias voltages up to 100 V were applied and the current was simultaneously measured via a SourceMeter 2410 from Keithley.

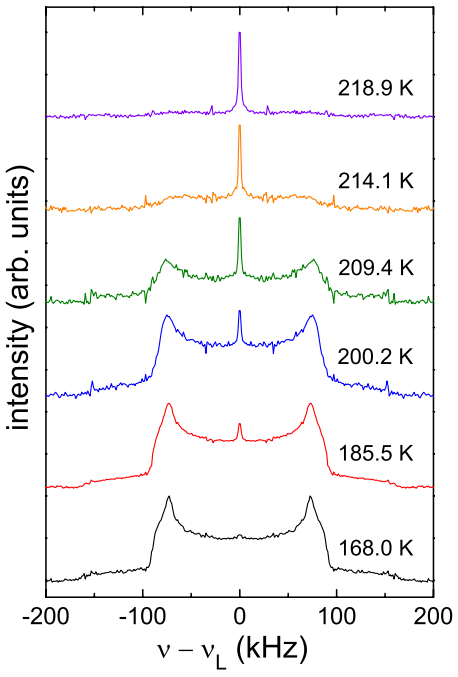

FIG. 1. (Color online) Solid-echo spectra of an $x = 10^{-4}$ KOH doped $THF \cdot 17D_2O$, i.e., lattice-deuterated crystal as measured for a pulse separation of $\Delta = 20\ \mu s$. The spectra are all normalized to the same maximum amplitude.

III. RESULTS AND ANALYSES

A. Host dynamics

1. Solid-echo spectra

In order to monitor the dynamics of the water molecules on the clathrate hydrate lattice we recorded deuteron NMR solid-echo spectra for KOH-doped $THF \cdot 17D_2O$. The results shown in Fig. 1 refer to a sample with a KOH doping level of $x = 10^{-4}$. At high temperatures, the rapid D_2O dynamics gives rise to motionally narrowed spectra. Upon cooling broad spectral features develop and for temperatures below about 200 K the central spectral component successively vanishes, until a Pake-like powder pattern is established. For a quantitative description let us note that the quadrupolarly perturbed resonance frequencies are given by

$$\omega_Q = \pm \tfrac{1}{2}\delta(3\cos^2\theta - 1 - \eta\sin^2\theta\cos 2\phi). \qquad (1)$$

Here θ and ϕ specify the orientation of the deuteron EFG tensor in an O-D (or C-D) bond with respect to the laboratory frame in the usual manner and δ and η are the anisotropy and the asymmetry parameters, respectively.[26] From the spectrum shown in Fig. 1 for $T = 168$ K we find $\delta = 3e^2qQ/(4\hbar) = 2\pi \times 162$ kHz and $\eta = 0.1$. For clathrates with somewhat different doping levels similar values were

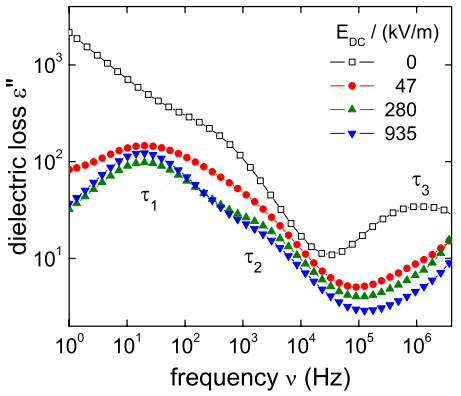

FIG. 2. (Color online) Dielectric loss spectra of $THF \cdot 17D_2O$ doped with $x=5\times10^{-4}$ KOH measured at 150 K. The curve labeled 0 kV/m is a reference spectrum which shows a loss peak maximum at 1 MHz and a strong dielectric low-frequency loss due to electrical conductivity. The three other sets of data were acquired after electrical cleaning at 263 K employing the given voltage levels. The field-treated samples no longer display the peak at 1 MHz and furthermore the conductivity loss is reduced to an extent that enables one to observe two additional relaxation processes unambiguously.

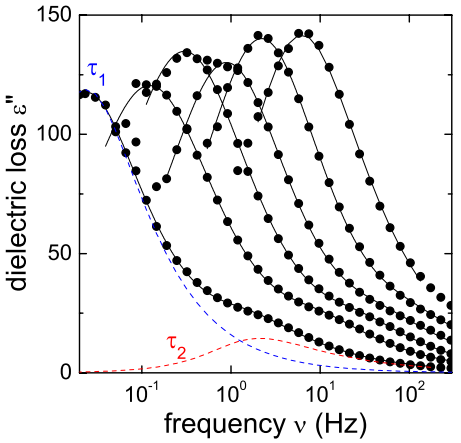

FIG. 3. (Color online) Dielectric loss spectra of $THF \cdot 17D_2O$ ($x=5\times10^{-4}$) as measured after electrical cleaning at 260 K. From left to right the measuring temperatures were 110, 120, 130, 135, 140, 145, and 150 K. The solid lines are fits using the Havriliak-Negami expression, Eq. (2), and the parameters given in the text or in the Arrhenius plot, Fig. 4. To illustrate the superposition of the two contributions, the parts of Eq. (2) corresponding to τ_1 and τ_2 are shown separately as dashed lines for the loss spectrum at $T=110$ K.

found (not shown). The spectra presented in Fig. 1 reveal a "two-phase" character which was reported to occur also for undoped clathrates.[3,27] A comparison with those earlier results shows that the broad and the narrow contributions evolve in similar temperature ranges. The integrated intensities of the two spectral components are of equal weight at a temperature near 220 K, at which the characteristic time scale is about $\delta^{-1}=0.98$ μs. Similar information can be obtained from measurements of the spin-spin relaxation time T_2 (not shown) which exhibits a minimum also at 220 K. The short T_2 values near this temperature are responsible for the reduced signal to noise ratio of some of the spectra shown in Fig. 1.

At temperatures near and below 170 K, a broad Pake-like pattern has fully emerged, indicating that the motional correlation times τ are much larger than δ^{-1}. Hence, the NMR spectra presented in Fig. 1 for $x=1\times10^{-4}$ do not provide signs of a KOH induced acceleration of the proton dynamics. Such an acceleration, with time scales ≤1 μs for $T>100$ K was reported from dielectric measurements at a slightly higher doping level ($x=1.8\times10^{-4}$) (Ref. 6) and would lead to an at least partial motional narrowing of the deuteron NMR spectra.

2. Dielectric relaxation, electrical conductivity, and ion sweeping

The earlier dielectric observation[6] of a dramatic increase of the dynamics with respect to the undoped clathrates was confirmed in the course of the present work for samples with $x=5\times10^{-4}$ and $x=1\times10^{-3}$. Corresponding data acquired at 150 K are shown in Fig. 2 for $x=5\times10^{-4}$ as open symbols. They indicate a dielectric loss peak at a frequency of $\nu_{max}=1$ MHz corresponding to a time scale of $\tau_3=1/(2\pi\nu_{max})=0.16$ μs. At frequencies $\nu\ll\nu_{max}$ large losses due to a strong electrical conductivity are present. These effects mask any relaxation processes, which might occur in this range. A unique $\varepsilon''\propto\sigma_{DC}/\nu$ behavior is not observed in the experimental frequency window for this sample. This precludes a simple subtraction of the dc conductivity, σ_{DC}, from the data, a procedure sometimes employed to make "hidden" relaxation processes visible.

However, with a recently revived dielectric cleaning technique,[25] we were able to reduce the effective electrical conductivity significantly and to uncover additional relaxation peaks. The experimental procedure was as follows: After solidifying a doped clathrate hydrate solution a reference spectrum was recorded at 150 K. Subsequently, the sample was heated to 263 K and subjected to an electrical bias field E while simultaneously monitoring the electrical current flowing through the sample. Depending on the run, the E field ranged from 47 to 935 kV/m. After about 10 min the current settled in the sub-mA range indicating that a dynamical equilibrium was reached. Then, the sample was cooled to 150 K, at which the current dropped to below 10 pA, the bias voltage was switched off, and dielectric data were taken. The closed symbols in Fig. 2 reflect the results of three independent runs, i.e., each measurement started from 260 K. The existence of two relaxation processes is clearly seen, at least for $E\geq280$ kV/m.

These processes were monitored as a function of temperature. Results for a clathrate hydrate doped with $x=5\times10^{-4}$ KOH are presented in Fig. 3. For a quantitative analysis of the results we employed a superposition of two Havriliak-Negami functions

$$\varepsilon''=\mathrm{Im}\left\{\sum_{k=1}^{2}\frac{\Delta\varepsilon_k}{[1+(2\pi i\nu\tau_k)^{\alpha_k}]^{\gamma_k}}\right\}. \quad (2)$$

Here the index k refers to the relaxation peak showing up at lower ($k=1$) or higher frequencies ($k=2$). The processes are

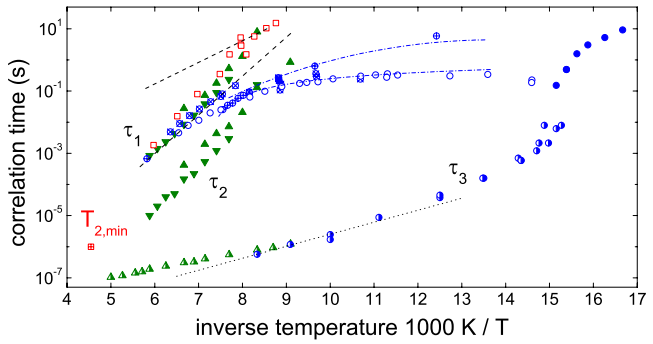

FIG. 4. (Color online) Arrhenius plot of various time scales of KOH doped clathrate hydrate samples. The correlation times are represented as closed or half-filled symbols (dielectric results) and open or crossed symbols (NMR data). The squares (red in the online version), triangles (green), and circles (blue) correspond to KOH-contents of $x=1\times10^{-4}$, 5×10^{-4}, and 1×10^{-3}, respectively. The crossing or half filling of symbols is used to distinguish different samples with the same nominal composition. The dotted line reflects an Arrhenius law with an activation energy of 7.4 kJ/mol as reported from dielectric measurements on a sample with $x=1.8\times10^{-4}$, see Ref. 6. The dashed lines reflect NMR data on undoped samples from Ref. 27. The dashed-dotted lines are drawn to guide the eye.

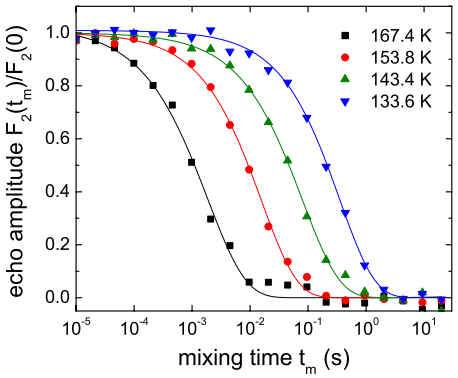

FIG. 5. (Color online) Mixing time dependent stimulated-echo intensities $F_2(t_m)$ for $x=10^{-4}$ KOH-doped THF·17D_2O are shown as symbols. The solid lines are fits using a stretched exponential function, Eq. (4). The stimulated-echo data were recorded for an evolution time of $t_p=20$ μs.

characterized by dispersion strengths $\Delta\varepsilon_k$. The shape parameters α_k and γ_k account for the width and the asymmetry of the dielectric loss profiles. The solid lines in Fig. 3 represent fits using Eq. (2) and yielded $\alpha_1=0.78\pm0.04$, $\gamma_1=1$ and $\alpha_2=1$, $\gamma_2=0.51\pm0.02$ corresponding to loss spectra with a full width at half maximum (FWHM) of 1.7 and 1.6 decades, respectively. The ratio of dispersion strengths of processes 1 and 2 turned out to be $\Delta\varepsilon_1/\Delta\varepsilon_2=9.9\pm0.8$. From a measurement of a second sample of identical composition a similar ratio was found. This statement also holds for the relaxation times, which are shown in an Arrhenius plot, see Fig. 4. Here a ratio $\tau_1/\tau_2=67\pm15$ was determined for the slower relaxations of the two samples. Thus, together with the fastest relaxation, which we will term process 3, at a given temperature up to three processes could be identified. It should be noted, however, that subsequent to the application of the electrical cleaning procedure, a peak associated with this latter process is no longer detectable.

3. Slow motions monitored by stimulated echoes

The range of time scales that is available through our dielectric measurements roughly coincides with that in which three-pulse stimulated-echo NMR experiments permit direct access to the ω_Q-modulated echo intensity

$$F_2(t_p,t_m)=\langle\cos[\omega_Q(0)t_p]\cos[\omega_Q(t_m)t_p]\rangle. \quad (3)$$

The corresponding correlation function enables one to detect motional processes on the time scale of ms…s. The time intervals t_p and t_m appearing in Eq. (3) are called evolution time and mixing time, respectively. Typically, by varying t_m one can find out how fast the O-D (or C-D) bonds reorient, i.e., in the present situation, what the reorientational correlation time τ of the water molecules is. By adjusting t_p the sensitivity of the experiment can be varied: the larger t_p is chosen with respect to the inverse anisotropy parameter, the smaller are the reorientation angles that are necessary to lead to a decay of F_2.

In Fig. 5, we show experimental data for an $x=10^{-4}$ sample for several temperatures with $t_p=20$ μs kept fixed. One sees that the molecular dynamics slows down upon cooling, but that the shape of the decay function remains invariant within experimental error. For a quantitative analysis we used the stretched exponential function

$$F_2(t_p,t_m)=A_1+A_2\exp[-(t_m/\tau)^{\beta}]. \quad (4)$$

Here, β is a phenomenological parameter which quantifies the deviations from a simple exponential relaxation. A_1+A_2 and A_1 are the limiting values of F_2 for short and long mixing times, respectively. The final state amplitude $Z\equiv A_1/(A_1+A_2)$ can provide information about the number, Z^{-1}, of magnetically distinguishable orientations that an O-D bond can attain.

After taking into account the independently measured spin-lattice relaxation times,[28] least-squares fits of F_2 based on Eq. (4) yielded $\beta=0.69\pm0.05$ and $Z\approx0$ for the temperature range which is shown in Fig. 5. The latter means that a large number of orientations in accessible for the O-D bonds. Hence, this process seems to be analogous to the slow process in the pure THF clathrate hydrate[27] which was shown to be associated with a long-range proton motion. Via rotational-translational coupling a large number of orientations is visited in the course of this motion. Without doping F_2 decays exponentially,[27] hence the stretched behavior which is observed here arises from the presence of defects and their statistical spatial distribution.

The time constants τ resulting from the fits to the NMR data are included in Fig. 4. They are compatible with the dielectric relaxation times τ_1 obtained after electrical cleaning. Stimulated-echo measurements were also performed for a sample with $x=10^{-3}$. Again, a single correlation decay is observed at high temperatures, yielding time constants which agree with τ_1 for $T>125$ K, see Fig. 4. Below 125 K the correlation times for samples with $x=10^{-3}$ tend to saturate.[29]

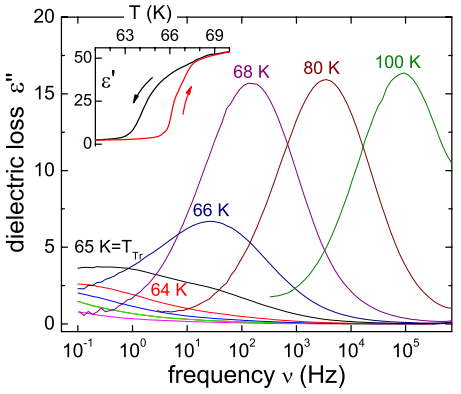

FIG. 6. (Color online) The lines represent dielectric loss spectra of 10^{-3} KOH-doped THF·17D_2O above and slightly below the phase transition which reveals itself via a drop of the loss peak maximum. The inset depicts the hysteresis associated with the first-order phase transformation which was measured via the dielectric constant at a frequency of 20 Hz by ramping the temperature with a cooling/heating rate of ± 0.3 K/min.

A second, faster process which would correspond to τ_2 was not detected for the sample with $x=10^{-4}$. Fast motions could be observed for more heavily doped samples. However, their time scales (at 100 K in the range from 10^{-4} to 10^{-2} s) and relative amplitudes show large variations from sample to sample, for reasons which are unknown at present.

B. Monitoring the order/disorder phase transition

In contrast to the undoped THF clathrate hydrates a phase transition can be observed in sufficiently strongly ($x \geq 1.8 \times 10^{-4}$) KOH doped clathrates. This phase transition affects the host as well as the guest dynamics and can be monitored using DS and NMR.

1. Dielectric detection

Fig. 6 documents dielectric loss spectra of a $x=10^{-3}$ sample which were recorded upon heating through a temperature range close to the phase transition. Above about 65 K the dielectric loss peak maximum increases steeply signaling that a transition takes place from a phase with minor or no dipolar mobility into one characterized by a significant amount of motion. For $T \geq 64$ K the peak frequencies could be read off directly from Fig. 6. For lower temperatures the peak frequencies were estimated from the shift factor required to construct a master plot on the basis of the dielectric loss. The resulting time constants are included in the Arrhenius plot, see Fig. 4, and indicate a jump in τ near 65 K.

For a first-order phase transition one expects to observe hysteresis upon temperature cycling and this expectation is indeed confirmed in the present case as the inset of Fig. 6 shows. Here, we plot the temperature dependent dielectric constant for the lowest measuring frequency utilized during this specific run. The hysteresis (recorded at a ramping rate of 0.3 K/min) amounts to $\Delta T \approx 2.3$ K around a midpoint temperature of 65.1 K. Based on the calorimetric measurements mentioned in the Introduction, it was reported that the ordering in the low-temperature phase, which comprises both host and guest degrees of freedom, is incomplete to an extent that is not exactly known.[13] With the current approach it is also not possible to quantify the order parameter of the lattice. However, the degree of order exhibited by the guest molecules will become accessible by the experiments described in Sec. III C 2, below.

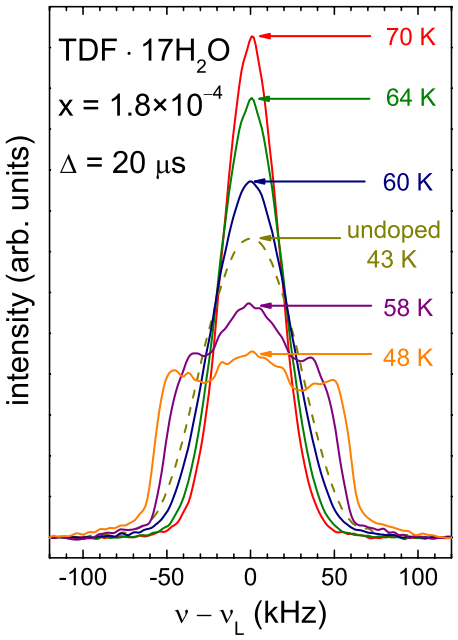

FIG. 7. (Color online) Solid-echo spectra of an $x=1.8 \times 10^{-4}$ KOH doped, guest-deuterated TDF·17H_2O crystal as measured for an echo delay of $\Delta=20$ μs are represented as solid lines. The spectra are normalized to exhibit the same integrated intensity. Upon cooling to below the phase transition temperature the spectra change abruptly from a bell shape to a more structured profile. The dashed line represents measurements from an undoped TDF·17H_2O crystal, taken from Ref. 20.

2. Phase transformation revealed by NMR

From NMR investigations on pure THF clathrate hydrates it is known that the guest dynamics is much faster than that of the host lattice.[19] On the timescale of the inverse Larmor frequency, i.e., in the range of nanoseconds, the slow-down of the THF molecules occurs near 50 K in the undoped crystal.

The dynamics of the THF guests was studied for a powdered TDF·17H_2O crystal with $x=1.8 \times 10^{-4}$. In Fig. 7 we show temperature dependent spectra for this sample. At temperatures above 60 K the spectra exhibit a Gaussian shape and below this temperature a markedly different line profile is obtained. The abrupt spectral change observed just below 60 K is the hallmark of the transition into a (partially) proton-ordered state. Figure 7 includes also a spectrum from an undoped crystal acquired at a temperature of 43 K.[20] One has the impression that it looks like a spectrum that would have shown up for the doped sample just below the phase transition—if this transition had not intervened. This apparent shift of temperature scale is confirmed by a quantitative

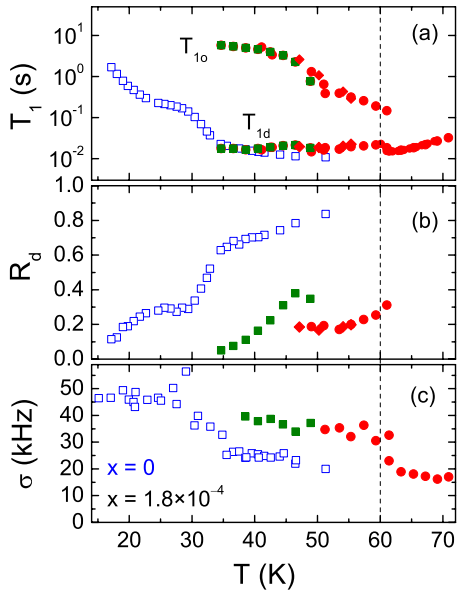

FIG. 8. (Color online) (a) Spin-lattice relaxation times T_{1o} and T_{1d}, (b) weighting factors R_d, and (c) square root σ of the second moment of the NMR spectra as a function of temperature. The open symbols refer to pure TDF·17H_2O (data taken from Ref. 20) and the filled symbols to a crystal doped with 1.8×10^{-4} KOH (this work). The different closed symbols refer to runs carried out for different thermal histories as described in the text (slower cooling, run A: ● and run B: ◆, as well as faster cooling, run C: ■). While R_d depends significantly on how fast the sample was cooled into the low-temperature phase, the numerical value of T_1 is practically unaffected by the thermal history. The dashed line indicates the midpoint of the phase transition. Due to hysteretic effects two different values occur at some temperature near the transition.

analysis for which we calculated the standard deviation $\sigma = \sqrt{\int I(\omega)\omega^2 d\omega / \int I(\omega) d\omega}$ from our NMR spectra. Here $I(\omega)$ designates the frequency dependent spectral intensity. The results for the width parameter σ are collected in Fig. 8(c). It is evident that $\sigma(T)$ varies discontinuously near the phase transition temperature. Otherwise, the $\sigma(T)$ pattern seen in Fig. 8(c) resembles that of the undoped system. However, it appears up-shifted by more than 20 K along the temperature axis.

From these observations it is clear that the Gaussian line shape is the signature of the disordered phase. The extent to which this phase disappears is reflected by the decrease in the unstructured contribution to the line shape. This result confirms our previous modeling of the Gaussian line shapes in terms of a jump model, which takes into account that the guest motion is sensitive to the proton disorder on the water lattice.[20]

The hysteresis of the phase transition was also checked via the spin-lattice relaxation of the guest molecules. In this context it is important to point out that above the phase transition temperature the longitudinal magnetization recovery, $M(t)$, was almost exponential but below this temperature it involved a slow and a fast component. As will become obvious in Sec. III C 1, below, these components refer to the ordered and the disordered regions of the sample, respectively. To record a full $M(t)$ curve may be quite time consuming. But in order to monitor the amount, e.g., of the disordered phase semiquantitatively with a high-temporal resolution it suffices to detect $M(t_d)$ at a fixed time interval t_d after saturation.[30] To this end t_d was chosen such that essentially only the faster spin-lattice relaxation component contributes to the signal.

By cycling the temperature from 65 to 39 K and back with a mean rate of 1.5 K/min the midpoint of the transition turned out to be at 60.0 K and the total width of the hysteresis was $\Delta T = 2.3$ K. This temperature agrees well with the transformation temperature of 61.9 K from calorimetry,[12] but it is somewhat smaller than 65.1 K as found for the lattice-deuterated crystals (cf. Sec. III A 2). The isotope-induced temperature shift of 5.1 K can be compared with the one implied by reports on KOH doped H_2O and D_2O which order at 72 and 76 K, respectively.[31]

C. Guest dynamics below the phase transition

1. Spin-lattice relaxation

As just noted, below the phase transition temperature the spin-lattice relaxation turns bimodal. The corresponding spin-lattice relaxation times are designated T_{1o} (referring to ordered) and T_{1d} (referring to disordered) so that the time dependent part of the magnetization can be described by

$$M(t) = M_0\{(1-R_d)\exp[-(t/T_{1o})^{1-\nu_o}] + R_d \exp[-(t/T_{1d})^{1-\nu_d}]\}. \quad (5)$$

Here M_0 is the maximum signal amplitude, the ν-exponents characterize the nonexponentiality of the magnetization build-up after saturation, and R_d measures the fraction of the component which relaxes faster. The parameters resulting from the fits to our data on a crystal with $x=1.8\times10^{-4}$ are included in Fig. 8. In frame (a) the relaxation time of the fast component, T_{1d}, is seen to be practically temperature independent, keeping more or less the numerical value observed just above the phase transition. This indicates that T_{1d} might correspond to those THF molecules which remain disordered, even below the phase transition temperature. The other component, which just below the phase transition is about one order of magnitude longer, increases significantly upon lowering the temperature and then saturates. By comparison with the mean spin-lattice relaxation times of the undoped sample, T_{1o} appears to be shifted to higher temperatures and also to larger values.

For the stretching exponent ν one has to distinguish three temperature intervals. Above the transition temperature $M(t)$ is close to single exponential with $\nu=0.05$. Directly below the transition ν_d and ν_o differ significantly. Whereas the longitudinal relaxation of the disordered state remains exponential with a stretching parameter ν_d close to 0, ν_o is around 0.5. Below 48 K the two stretching exponents exhibit the same value of about 0.25.

The assignment of the components to the ordered or to the disordered component has been checked by measuring NMR spectra for various waiting times t_w subsequent to the saturation of the longitudinal magnetization. For small t_w only the components associated with short T_1 times will contrib-

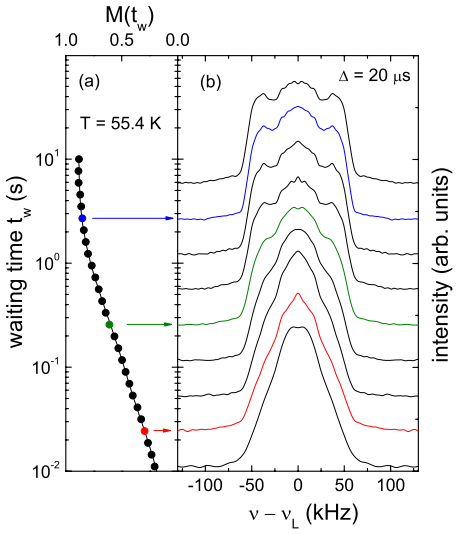

FIG. 9. (Color online) (a) Magnetization recovery as a function of the waiting time t_w and (b) solid-echo spectra measured at a time t_w after the saturation of the magnetization for a TDF·17H_2O crystal with $x=1.8\times10^{-4}$. The spectra are all normalized to the same maximum intensity. The base lines of the spectra correspond to the waiting times that are highlighted for a few t_w by different colors and arrows in frame (a). The solid-echo pulse separation was $\Delta=20$ μs.

ute to the spectra. With increasing t_w the equilibrium spectra which comprise all contributions will successively emerge. Corresponding experimental results taken somewhat below the phase transition temperature are shown in Fig. 9. For small t_w only a broad Gaussian-like line shape, characteristic of the disordered phase, is observed. For longer t_w one recognizes how a Pake-like pattern becomes superimposed onto the unstructured central feature. These results are clear evidence for the assignments implied above.

Let us now discuss the temperature dependence of the relative weight of the T_1 components. In Fig. 8(b), we present the contribution of the disordered part, R_d, which was obtained under various experimental conditions. In two runs (called run A and run B) we cooled the crystals slowly (≈-0.03 K/min and ≈-0.14 K/min) through the phase transition and observed that R_d is about 0.2 for 48 K$\leq T\leq$60 K. In another run (run C) we quenched the crystal (≈-0.63 K/min) to about 50 K and obtained a significantly larger value, $R_d\approx0.35$. When slowly cooling the sample further ($\approx3.5\times10^{-4}$ K/min), the relative weight of the faster component decreased successively, see Fig. 8(b), and below about 35 K it became almost undetectable. In yet another measurement we cooled the sample quickly through the phase transition (≈-1.1 K/min) and after stabilizing the temperature near 55 K, we observed that the magnetization of the fast component decreased by about 12% within a time interval of 17 h (not shown).

We also performed spin-spin relaxation measurements for 48 K$\leq T\leq$60 K and found a bimodal transversal dephasing (not shown). The longer component, $T_{2d}=(600\pm100)$ μs, is compatible with the values of the undoped sample which is in the disordered state. For the other component we find $T_{2o}=170$ μs just below the phase transition, then T_{2o} continuously shortens reaching 100 μs at 48 K.

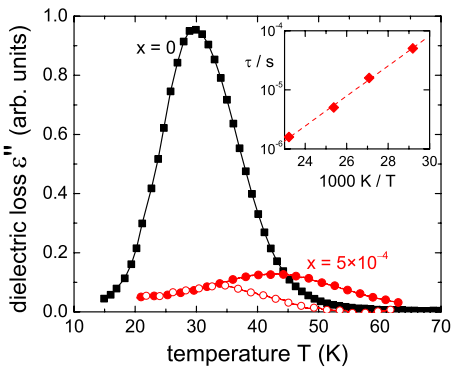

FIG. 10. (Color online) Reorientation dynamics of the mobile guests in the low-temperature regime as measured upon heating. The dielectric loss of an undoped sample (squares) is compared with data for a crystal with $x=5\times10^{-4}$ (circles). The measuring frequencies are 1 kHz (open symbols) and 100 kHz (closed symbols). The inset shows an Arrhenius representation of the loss peak frequencies of the doped sample. The dashed line reflects an energy barrier of 585 K or 4.9 kJ/mol.

2. Reorientations in the low-temperature phase

In KOH-doped ice[7,31] and similarly for the doped clathrate hydrate[6] the low-temperature proton ordering is not complete. Therefore, one may ask whether for $T<T_c$ the disordered cages or regions in the sample are still dynamically active, in other words, whether the guest molecules can reorient on the time scales accessible with the present experiments. Indeed from NMR measurements on the crystal with $x=1.8\times10^{-4}$, which was rapidly cooled to 45 K and a few Kelvin below, we obtain a short-time decay of F_2. The effective time constants are in the range of 140 μs at 44.5 K to 600 μs at 38.5 K (not shown), but the real values are likely to be somewhat shorter.[32] Unfortunately the associated spin-lattice relaxation times are relatively short [$T_1\approx10$ ms, see Fig. 8(b)] so that the measurements could only be performed in a narrow temperature range.

A more satisfactory determination of time scales was possible using dielectric spectroscopy. The corresponding dielectric losses are shown in Fig. 10 for an undoped THF·17H_2O and a KOH-doped THF·17D_2O clathrate hydrate sample. The time constants determined from the peak maxima of the doped sample recorded at several frequencies are indicative for a thermally activated process, see the inset of Fig. 10. Its energy barrier is roughly the same as the one characteristic for the slow-down of the guest dynamics in undoped THF-clathrate hydrate.[4,20,33] However, the time scales obtained from the data in Fig. 10 are about 100 times longer. Taking the peak amplitudes as a rough estimate for the number of mobile guests, Fig. 10 shows that in the doped sample their fraction is not larger than about 10–12%.[34] A similar fraction of guests in disordered environments was inferred from our NMR measurements, see Fig. 8(b). This leads us to conclude that also dielectric spectroscopy monitors only the molecules in the disordered regions. In other words, the motions of the guests located in proton-ordered regions are not detectable in the frequency window of our dielectric measurements. Furthermore, the time scale factor

of about 100 implies that the presence of the proton-ordered regions slows the dynamics in the disordered domains significantly.

IV. DISCUSSION

One recurring observation made in the course of the present study is that the reproducibility of the results was not always as good as we are used to from our studies on undoped clathrates. Repeat runs usually gave at least qualitatively the same results but they did not always reproduce quantitatively. Hence, some parameters could not be determined reliably (e.g., the time constants from dielectric measurements on nominally identical samples, see Fig. 4) or some observations did not appear fully systematic (see, e.g., the crossing of some of the dielectric loss curves for different cleaning voltages in Fig. 2). This somewhat disturbing feature of the present work is not without precedence. In heavily doped ices similar observations have been made and were ascribed to the hard-to-control distributions of ions, domain walls etc.[7] which may arise from very slight, undesired, and hard-to-control differences in the sample preparation.

A. Comparison with KOH doped ice

To understand better the behavior of KOH-doped clathrate hydrates it is worthwhile to make some comparison with KOH doped ice I_h. Here the K^+ ions are thought to be interstitially embedded into the crystal lattice[7] and each OH^- defect can liberate an *L*-defect, i.e., an 'empty' hydrogen bond. These defects can be visualized as breaking the Bernal-Fowler ice rules locally thereby speeding up the proton dynamics. It has been stated that each dopant molecule can generate an activated region that involves about 10^4 water molecules.[35] In these domains the dynamics is apparently accelerated to an extent which facilitates the establishment of proton order at low temperatures. Results from neutron scattering indicated that the spatial dimension of the proton ordered regions, which presumably emerge from the activated domains, is smaller than 40 nm.[36]

If the degree of ordering depends on the amount of doping, in the sense that below a certain level no ordering occurs, and with the limited solubility of KOH in ice ($x \leq 10^{-3}$), the random spatial distribution of the defects precludes that usually the entire sample is activated. As a consequence an only partial order emerges at low temperatures.[37] Its slow establishment in the laboratory[38] has been related to the time it requires to reorganize disordered regions that are trapped between differently oriented ordered domains.[39]

Viewing, in a simplified manner, the clathrates as an ice crystal with periodically embedded voids it becomes clear why many of their properties resemble those of ice if one plausibly assumes that the same microscopic mechanisms govern the dynamics of both types of substances. So what are the differences between them? It has been found that the dynamics in the doped clathrate hydrates is faster than in hexagonal ice, see, e.g., Fig. 11 in Ref. 35. This was interpreted to indicate that the presence of guests can induce further defects in the surrounding hydrate lattice.[17,40] Associating the less densely packed water lattice of the clathrates relative to that of ice with a dilution of the cooperative interactions mediated by the ice rules, the lower transition temperature in the clathrate can be rationalized. In both substances the transformation to the partially ordered state occurs upon cooling when the dynamics in the activated regions is in the range of 0.1…1 s (see, e.g., Ref. 41 or Fig. 4). Incidentally, from calorimetric experiments on *un*doped THF clathrate hydrate it follows that the extrapolated correlation time near 65 K could be at least as long as several weeks.[35]

At temperatures $T > 100$ K the dynamics of the fastest reorientational process of doped ice and of doped THF clathrate hydrate (see Ref. 41 or Fig. 4, respectively) is very weakly thermally activated. In other words, it exhibits an (almost) vanishing activation energy. For ice I_h this observation was ascribed to an (almost) temperature independent mobility of the OH^- defects while at temperatures below 100 K these ionic defects become increasingly trapped.[41] Consequently, in Ref. 41 it was argued that sufficiently far below the melting point *L*-defects cease to contribute significantly to the dynamics in ice I_h.

B. Nature of the relaxation processes related to the host lattice

Previous dielectric measurements provided evidence for just a single slow relaxation process in pure THF clathrate hydrate as well as a single, much faster relaxation process in the KOH doped system.[6] However, by employing large electrical fields for doped specimens we were able to detect up to three relaxation processes at a given temperature.

The fastest of them (process 3) coincides with that detected in previous dielectric experiments[6] and regarding its origin it is interesting to reconsider the data shown in Fig. 2: The sample which has not undergone a bias field treatment shows a loss peak at about 1 MHz. However, following the cleaning procedure this feature has vanished and did not reappear in the experimental frequency window upon cooling the sample. This finding can be interpreted as follows: At 260 K, i.e., only about 15 K below the melting point of the system, at which the large electrical field is applied, any mobile ionic species are precipitated to the electrodes. With far less ionic impurities in the bulk of the sample, at lower temperatures the ionic conductivity is dramatically suppressed, in accord with our observations, see Fig. 2. More importantly, the number of ionic centers which can facilitate dipolar rearrangements in the activated regions is then strongly reduced. The NMR detection of a fast process is so far not without ambiguity, see the remarks made near the end of Sec. III A 3, and calls for further study.

Regarding the two slower relaxations it is instructive to point out that also for undoped THF clathrate hydrates two processes were detected. The faster of them (corresponding to τ_2) has been demonstrated via stimulated-echo NMR to arise from on-site tetrahedral jumps of the D_2O molecules, while the slower process (corresponding to τ_1) has been reported to involve also translational jumps of the water molecules.[27] The temperature dependences of the correlation time constants from Ref. 27 are schematically included in

Fig. 4, see the dashed lines. The relaxation processes that we observe for the doped crystal show similar temperature dependences, however, they are shifted to somewhat shorter time scales. Since, the impurity-induced speed up of the dynamics in icelike phases is well known, and since the presence of the guests creates further defects on the hydrate lattice,[40] this strongly suggests to view the two slow processes in the doped samples as the pendants of those observed in the pure system.

V. SUMMARY AND CONCLUSIONS

Using dielectric spectroscopy and deuteron NMR we studied (1) the jump processes of the water molecules on the host lattice, (2) the fast KOH-induced defect dynamics which triggers the transformation to the ordered low-temperature phase, as well as (3) the reorientational motion of the THF guests in that phase. Our main results can be summarized as follows:

Like in the undoped THF clathrate hydrate the slow dynamics on the host lattice involves two processes. These are compatible with an assignment in terms of a faster on-site reorientational and an about 70 times slower translation-mediated reorientational process. By suitable electric field treatment these processes were rendered visible using dielectric spectroscopy. The activation energy of the slower process is about 28 kJ/mol. If the KOH doping level is larger than 10^{-4}, its effective jump rate tends to saturate for $T < 100$ K. The near temperature independence of the slowest process is reminiscent of NMR results on undoped THF clathrate hydrate.[2] While our dielectric results and the NMR determination of the slower process were quite reproducible, the strength and time constant governing the faster process was subject to major sample-to-sample variations. Since they appeared also for the same nominal KOH-contents and for virtually identical sample handlings, it is suspected that a varying spatial distribution of the defects could play a role.

The phase transition appearing in the samples doped at levels $x > 10^{-4}$ was observed using dielectric spectroscopy and by monitoring the guest dynamics via NMR. At temperatures not too far below the transition temperature, the residual degree of guest order is in the 10–20% range, so that the reorientational motion of the dynamically disordered THF molecules could be detected. Thus, an ordering of the lattice also leads to a freeze-out of the guests, emphasizing the importance of the host-guest interactions. Overall our study shows that KOH-doped clathrate hydrates bear a close similarity with KOH doped hexagonal ice, except that due to the presence of guests the clathrates offer additional means to study the hydrate dynamics.

ACKNOWLEDGMENT

We thank F. Förster and M. Heikenfeld for carrying out preliminary dielectric measurements on doped clathrates. The funding of this work by the Deutsche Forschungsgemeinschaft under Grant No. Bo1301/7-1 is gratefully acknowledged.

*roland.bohmer@tu-dortmund.de

[1] E. D. Sloan, Nature (London) **426**, 353 (2003).
[2] T. M. Kirschgen, M. D. Zeidler, B. Geil, and F. Fujara, Phys. Chem. Chem. Phys. **5**, 5243 (2003).
[3] M. Bach-Vergés, S. J. Kitchin, K. D. M. Harris, M. Zugic, and C. A. Koh, J. Phys. Chem. B **105**, 2699 (2001).
[4] S. R. Gough, R. E. Hawkins, B. Morris, and D. W. Davidson, J. Phys. Chem. **77**, 2969 (1973).
[5] H. Suga, T. Matsuo, and O. Yamamuro, Pure Appl. Chem. **64**, 17 (1992).
[6] O. Yamamuro, T. Matsuo, and H. Suga, J. Inclusion Phenom. **8**, 33 (1990).
[7] V. F. Petrenko and R. W. Whitworth, *Physics of Ice* (Oxford University Press, Oxford, 1999).
[8] F. Fujara, S. Wefing, and W. F. Kuhs, J. Chem. Phys. **88**, 6801 (1988).
[9] S. Kawada and R. Tutiya, J. Phys. Chem. Solids **58**, 115 (1997).
[10] S. Kawada, J. Phys. Soc. Jpn. **32**, 1442 (1972).
[11] C. G. Salzmann, P. G. Radaelli, A. Hallbrucker, E. Mayer, and J. L. Finney, Science **311**, 1758 (2006).
[12] O. Yamamuro, M. Oguni, T. Matsuo, and H. Suga, Solid State Commun. **62**, 289 (1987).
[13] O. Yamamuro, M. Oguni, T. Matsuo, and H. Suga, J. Phys. Chem. Solids **49**, 425 (1988).
[14] O. Yamamuro, T. Matsuo, H. Suga, W. I. F. David, M. Ibberson, and A. J. Leadbetter, Physica **213-214**, 405 (1995).
[15] A. I. Krivchikov, O. O. Romantsova, and O. A. Korolyuk, Low Temp. Phys. **34**, 648 (2008).
[16] In particular doped trimethylene oxide-, acetone-, and 1,4-dioxane-clathrate hydrates were studied, see O. Yamamuro, N. Kuratomi, T. Matsuo, and H. Suga, J. Phys. Chem. Solids **54**, 229 (1993).
[17] M. Tyagi and S. S. N. Murthy, J. Phys. Chem. A **106**, 5072 (2002).
[18] S. K. Garg, D. W. Davidson, and J. A. Ripmeester, J. Magn. Reson. **15**, 295 (1974).
[19] D. W. Davidson, S. K. Garg, and J. A. Ripmeester, J. Magn. Reson. **31**, 399 (1978).
[20] A. Nowaczyk, B. Geil, S. Schildmann, and R. Böhmer, Phys. Rev. B **80**, 144303 (2009).
[21] B. Geil, T. M. Kirschgen, and F. Fujara, Phys. Rev. B **72**, 014304 (2005).
[22] A. Steinemann, Helv. Phys. Acta **30**, 581 (1957).
[23] When annealing KOH doped THF clathrate hydrates for about one day at 260 K a low-temperature phase transition was no longer detectable, i.e., the samples behaved as if they were undoped.
[24] For measurements carried out at $T > 77$ K the $\pi/2$ length was 2.5 μs otherwise it was 5.5 μs.
[25] C. Gainaru, R. Böhmer, and G. Williams, Eur. Phys. J. B **75**, 209 (2010).
[26] K. Schmidt-Rohr and H. W. Spiess, *Multidimensional Solid State*

NMR and Polymers (Academic, London, 1994), p. 66.

[27] T. M. Kirschgen, M. D. Zeidler, B. Geil, and F. Fujara, Phys. Chem. Chem. Phys. **5**, 5247 (2003).

[28] For the THF·17D_2O sample with $x=10^{-4}$ the measured spin-lattice relaxation is practically exponential and virtually identical to that reported in Ref. 2. For samples with larger x and $T>100$ K T_1 is slightly stretched ($\nu \leq 0.1$) and in some cases reaches $T_1 \approx 14$ s at 150 K. This is ~16 times less than in the undoped sample.

[29] A very weak temperature dependence of the slower process was also reported for the pure clathrate hydrate, Ref. 27. Therefore, the slowest relaxation time in the doped system can possibly be viewed analogous to that process.

[30] This technique was used previously to characterize first-order phase transitions, see M. Winterlich, H. Zimmermann, and R. Böhmer, J. Non-Cryst. Solids **307-310**, 442 (2002).

[31] Y. Tajima, T. Matsuo, and H. Suga, Nature (London) **299**, 810 (1982).

[32] The interpretation of time constants τ from stimulated-echo experiments can become cumbersome if $\tau \gg t_p$ is not fulfilled, i.e., if significant dynamics occurs during $2t_p$. Then parts of the correlation function that are faster than about t_p may remain undetected.

[33] D. W. Davidson, Can. J. Chem. **49**, 1224 (1971).

[34] Provided the width of $\varepsilon''(\omega)$ would be the same for the two samples the loss peak amplitudes would directly reflect $\Delta\varepsilon \propto n(\mathrm{THF})\mu^2/T$ if the peaks would appear at the same temperature. However, compared to the undoped crystal the frequency-dependent spectra of the doped sample are somewhat broader and more importantly the peak maxima are shifted to higher temperatures (partly due to the use of heavy water). Taking both effects into account this will reduce the estimated fraction of mobile guests somewhat but certainly no more than about 30%.

[35] H. Suga, Proc. Japan Acad. B **81**, 349 (2005).

[36] A. J. Leadbetter, R. C. Ward, J. Q. W. Clark, P. A. Tucker, T. Matsuo, and H. Suga, J. Chem. Phys. **82**, 424 (1985).

[37] Ref. 5 reports a degree of ordering of 82%.

[38] In antarctic ice which has never become colder than 237 K a degree of proton order of up to 50% was reported by H. Fukazawa, S. Mae, S. Ikeda, and O. Watanabe, Chem. Phys. Lett. **294**, 554 (1998); However, see A. D. Fortes, I. G. Wood, D. Grigoriev, M. Alfredsson, S. Kipfstuhl, K. S. Knight, and R. I. Smith, J. Chem. Phys. **120**, 11376 (2004).

[39] A. V. Zaretskii, R. Howe, and R. W. Whitworth, Philos. Mag. B **63**, 757 (1991).

[40] S. Alavi, R. Susilo, and J. A. Ripmeester, J. Chem. Phys. **130**, 174501 (2009).

[41] See Chapter 5.4.3.4 of Ref. 7 and references cited therein.